# AN ABSTRACT OF THE THESIS OF

Tessa C. Artruc for the degree of Master of Science in Water Resources Engineering presented on May 5, 2020.

Title: Numerical Modeling of Lateral Erosion during Reservoir Drawdown.

Abstract approved:

_____

Desirée D. Tullos

Reservoir drawdown is a management technique increasingly used in maintenance of aging infrastructure, decommissioning dams, and to promote the flushing of fish and sediment to downstream reaches. Erosional processes in the reservoir may result in excessive delivery of sediment to downstream habitats and infrastructure, a critical long-term consideration. Typically, numerical models of the reservoir's geomorphic response have been limited to 1D incisional erosion without the incorporation of lateral widening. The effective design of drawdown operations via predictive modeling provides a missed opportunity to address concerns around sedimentation of reservoirs, controlling the outcomes of dam maintenance and removal, and mitigating the effects of sediment starvation downstream of dams. A numerical model was developed and simulated to examine how drawdown rate and grain size affect the rate, magnitude, and timing of lateral erosion in a reservoir. The incorporation of retrogressive bank erosion and groundwater drawdown in this model are two new contributions to address sequential slumping, which is expected to improve the accuracy of modeling lateral erosion.

Field measurements from the drawdown for Elwha Dam removal were coupled with five drawdown scenarios: Staged, Staged with Short drawdown increments, Staged with Long drawdown increments, Slow, and Rapid drawdown. These scenarios were then re-evaluated with coarse material to understand the

integrated impact of grain size and drawdown process. Three overarching effects of drawdown emerged from the numerical experiments: 1) Staged drawdowns can produce a range of erosion volumes depending on how long the drawdown phases are relative to the hold periods, dictating the generation of undrained or drained conditions; 2) the timing of erosion was directly related to the drawdown rate, creating a tradeoff between the amount of impact created and when the impact is produced; and 3) coarse material reduced the magnitude of erosion compared to fine material when the internal friction angle was greater than the bank slope angle. The inclusion of retrogression as an avenue for sequential block failures proved to be an important contribution as all fine-grained scenarios exhibited at least one time step with more than one failure. The duration of hold periods was found to be less important than the duration of drawdown, as the drawdown increment drives slope stability (e.g. undrained/drained conditions). As a majority of failures occurred under undrained conditions where cohesion is present, the shear strength provided under drained conditions highlights the ability to achieve slope stability.

Several aspects of lateral erosion were simplified or not included, such as the immediate transport of failed materials, no incorporation of vegetation, homogeneous bank sediment, de-coupled incision and widening, assumed drained and undrained conditions, and a limit of model simulation to pre-high flow events. In addition, no validation data were available for model verifications. The use of high-frequency bathymetry surveys or estimations of bank retreat through UAV surveys could be used to better understand the processes behind lateral erosion with quantitative pre- and post-drawdown data. Further work with this model could focus on its integration into an existing hydrodynamic model for more accurate predictions of the magnitude, rate, and timing of lateral erosion. Due to the complexity of sediment transport both spatially and temporally, comprehensive models of both fluvial and geotechnical processes are crucial in understanding the interconnected impact of drawdown operations.

# Numerical Modeling of Lateral Erosion during Reservoir Drawdown

by
Tessa C. Artruc

A THESIS

submitted to

Oregon State University

in partial fulfillment of
the requirements for the
degree of

Master of Science

Presented May 5, 2020
Commencement June 2020

Master of Science thesis of Tessa C. Artruc presented on May 5, 2020

APPROVED:

Major Professor, representing Water Resources Engineering

Director of the Water Resources Graduate Program

Dean of the Graduate School

I understand that my thesis will become part of the permanent collection of Oregon State University libraries. My signature below authorizes release of my thesis to any reader upon request.

Tessa C. Artruc, Author

# ACKNOWLEDGEMENTS

I want to express my appreciation to my advisor, Desirée Tullos, for her unwavering patience in tackling all of the obstacles this project presented and reminding me why this work is so exciting. I would like to thank Ben Leshchinsky for walking me through the bones of this code and providing invaluable insight into bank stability. My thanks also goes to Jack Istok for digging into the civil engineering archives to find a groundwater solution. I'm incredibly grateful to Timothy Randle, Jennifer Bountry, Matthias Collins, and Andrew Ritchie, who have shared a lot of their time and data with me to explore the Elwha case study. I'm also appreciative to the administrators in the WRGP and BEE departments for keeping this academic ship afloat. Special thanks goes to Ron and Betty Miner, and to Bill and Jane Jackson for their financial support. This thesis also would not have been possible without my friends who made these two years so special. Lastly, I'd like to thank my family and Meghan for always supporting the dream.

# TABLE OF CONTENTS

TABLE OF CONTENTS (Continued)

# LIST OF FIGURES

# LIST OF TABLES

# LIST OF APPENDIX FIGURES

# 1. INTRODUCTION

Worldwide, sediment deposition in reservoirs leads to a loss of about 1% of storage capacity per year (Isaac and Eldho 2017), reductions in hydropower production, damaged power plant facilities, reduced quality of water, and erosive conditions downstream of the dam (Akbarizadeh et al. 2019). Future changes in climate have the potential to contribute large amounts of sediment to reservoirs (wildfires, flooding, glacial retreat), making sedimentation management increasingly important (Randle et al. 2017). Within the last 30 years, new dam and reservoir construction has not kept up with the reduction of storage due to sedimentation both in the United States and internationally, posing a serious threat to reliable water supplies (Randle et al. 2019). Approximately 200 reservoirs in California alone have lost more than half of their initial capacity to sedimentation (Minear and Kondolf, 2009). The impact of sedimentation can be contrasted spatially, with 60 feet of fill that plugged the water intake of Paonia Dam (Haung et al. 2019) or lost capacity that raised the water surface elevation two miles upstream from the original pool of the Cochiti Reservoir (Davis et al. 2014). In order to prevent the reservoir's storage capacity from being completely displaced, the sediment inflows and outflows must be balanced (Fan and Morris 1992). It is extremely difficult to replace sedimented reservoirs by developing new sites due to high costs, competition for resources, environmental obstacles, and lack of available sites.

Dam removal is an increasingly popular strategy to address the environmental impacts of dams and their increasing age in the U.S. (Doyle et al. 2002) and drawdown flushing is attracting increased attention globally for its ability to restore reservoir capacity and downstream sediment continuity (Kondolf et al. 2014). Drawdown involves lowering the reservoir pool elevation at critical times in hydrologic and ecological cycles. This can occur regularly as a management strategy (lowering and refilling the reservoir) or once as the base water level is permanently lowered during dam removal. Lowering of the water surface elevation initiates movement of the accumulated sediment within the reservoir, often resulting in

elevated delivery of sediment to downstream habitats, infrastructure, and coastal estuaries (Magilligan et al. 2016; Isaac and Eldho 2017; Randle and Bountry 2017).

Concern about the fate of the sediment in terms of reservoir erosion and downstream deposition is one of the biggest obstacles when implementing drawdown operations or designing dam removals (Doyle et al. 2002). Local structures or downstream ecosystems can be affected in unacceptable ways when incorrect predictions are made about the movement of the accumulated sediment. Most upstream infrastructure was also built assuming that the water and bed level of the channel was fixed, so vertical incision and subsequent channel widening may compromise the integrity of these structures (Doyle et al. 2002). Underestimated levels of suspended sediment due to poorly designed drawdown operations can have a direct impact of fish and macroinvertebrate mortality as well (Crosa et al. 2010; Espa et al. 2016).

Despite the critical need for reservoir management techniques like drawdown and the concern regarding the impacts of such actions, there is little to no basis in theory or empiricism to guide drawdown strategies. Since there is a knowledge gap between the outcomes of drawdown and engineering design, dredging operations are often proposed before drawdown or dam removal due to uncertainties (Cui and Wilcox 2008). It has been observed that the design and application of drawdown can influence the evolution of the impoundment and downstream transport of sediment. Randle and Bountry (2017) hypothesized that the effects from releasing a large volume of reservoir sediment downstream can be reduced by slowing the rate of reservoir drawdown. This process-based phase is driven by rapid incision and channel widening, which follow channel evolution models as a response to the lowered base level, increased water velocity, and mass wasting of impounded sediment (Pearson et al. 2011).

Typically, models of the reservoir's geomorphic response have been limited to one-dimensional incisional erosion without the incorporation of lateral widening (Foley et al. 2017; Cantelli et al. 2007; Pizzuto 2002). Some assume that channel width remains constant through time (Doyle et al. 2002), or that sediment transport is laterally uniform (Cui and Wilcox 2008). This creates a substantial knowledge gap in

erosion modeling, as the magnitude and rate of sediment eroded from the banks can be significant. For example, the Milltown Dam removal caused banks to migrate up to 200 meters (Epstein 2009), and the Marmot Dam removal observed lateral erosion rates up to 260 meters per day (Major et al. 2012). Thus, the exclusion of bank erosion can negatively influence erosion predictions, such as the one-dimensional model used for reservoir flushing on the Spencer Dam that underpredicted erosion by 43 percent (Gibson and Boyd, 2016). Existing bank stability models, such as the Bank Stability and Toe Erosion Model (BSTEM), have been used in two-dimensional models as an attempt to breach this gap (Lai 2014). However, some simplifying assumptions within these models leave room to improve on predictive modeling and explore broader questions. For example, BSTEM assumes a wedge failure, a friction slope equivalent to bed slope, and a hydrostatic groundwater level. The model does not simulate rotational failures that generally occur in very high banks of homogeneous, fine-grained materials characterized by low bank angles (Bankhead et al. 2013). Thus, there is room for improvement when simulating the complex sediment dynamics that occur due to drawdown operations.

Drawdown rate is expected to interact with the strength of reservoir sediments in a number of ways. In this study, the rate of drawdown (i.e. Rapid, Slow, Staged) is defined relative to the hydraulic conductivity of the sediment. Rapid drawdown is greater than the hydraulic conductivity, whereas Slow drawdown more closely matches the hydraulic conductivity. Lowered water level and excess pore water pressures are anticipated to greatly decrease the resisting forces of the soil mass and lead to geotechnical failure during the drawdown process. Water within a soil mass increases the pore water pressure, thus lowering the strength of the bank material (Reid 1992) and the overall factor of safety decreases. In a drawdown scenario, the external water level is lowered, reducing the normal force on the slope holding the bank profile in place (Doyle et al. 2003). However, these hypothesized interactions linking drawdown operations and lateral erosion have not been documented in the field or fully represented numerically with models.

The broad goal of this research is to more fully represent the erosional phenomena that occur during drawdown and evaluate how management scenarios

impact the lateral erosion produced by those phenomena. A numerical model was developed to fill gaps in current modeling approaches (e.g. retrogressive failure, dynamic groundwater levels), and then simulated to examine how (1) drawdown rate and (2) grain size affect the rate, magnitude, and timing of lateral erosion in a reservoir. Rate of erosion is calculated as the volume of erosion that occurs during one time step. Magnitude of erosion is calculated as the cumulative volume of erosion from the entire simulation. Timing of erosion is defined as the time step(s) at which erosional events occur. It was expected that drawdown rate and grain size would affect lateral erosion in the following ways:

1. Rapid drawdown will cause an increase in the volume and rate of lateral erosion relative to Slow drawdown. The elevated erosion is associated with mass wasting triggered by undrained sediment conditions that reduce internal friction, with failures occurring early in the simulation.
2. Slow drawdown will decrease the volume and rate of lateral erosion relative to Rapid drawdown due to the bank shear strength maintained by external water pressure, with failures occurring throughout the simulation
3. During phased drawdown, the rate of sediment evacuation is expected to depend on the phases of Staged drawdown. Staged drawdown with short drawdown phases is expected to increase the volume of mass wasting with earlier failures, when compared to Staged drawdown with long drawdown phases.
4. A larger grain size will decrease the volume and rate of erosion relative to the fine-grained scenarios, with failures occurring later in the simulation. The greater hydraulic conductivity and internal friction angle of coarser grains are expected to provide greater bank shear strength than fine materials.

To evaluate these expectations, field observations will be coupled with this model as a more representative example of true geometry, soil characteristics, and drawdown rate.

# 2. METHODS

## 2.1. Model Development

The objective of the model development was to represent the key processes associated with widening during drawdown, including new algorithms that highlight key factors associated with slope stability (Figure 1). Two bank erosion processes occur to induce lateral erosion: hydraulic erosion and geotechnical failure (Simon et al. 2000).

For the first process, hydraulic forces due to the change in friction slope and water depth erode the supporting base material at the toe of the bank and cause oversteepening of the slope (Simon et al., 2000). Hydraulic erosion is calculated with an excess shear stress approach, where erosion distance of an individual grain is a function of the difference between critical shear stress and boundary shear stress, as described in detail in Section 2.1.5.

For geotechnical failure, a variety of mechanisms contribute to bank instability. When the reservoir water level is high relative to the banks, the water acts as a confining force to provide bank stability and fully saturates the sediment. As the water level is lowered, the confining pressure from hydrostatic forces is lost, producing a discrepancy between the water in the channel (henceforth “external”) and water within the bank (henceforth “internal”)(Figure 2). Based on the drawdown scenario and sediment characteristics, the conditions of the bank sediments may be drained or undrained (Yu et al. 1998). Undrained conditions exist when the hydrologic conductivity of the sediment is insufficient to dissipate the excess pore water pressures developed and/or the loading is fast enough that non-hydrostatic pore water pressures develop (e.g. rapid drawdown of buttressing water)(Cetin and Cökoğlu, 2013)(Stark et al., 2005). Fine materials, such as the clays and silts of the reservoir, are typically undrained for some period of time after unloading due to their low hydraulic conductivity (Bernander et al. 1989). Coarse materials, such as the sands and gravels of the deltas, are typically under drained conditions due to the high hydraulic conductivity of those sediments (Rios et al., 2017). The effect of undrained conditions in reducing bank strength has long been identified as an important

contributor to streambank and hillslope instability (Simon et al. 2000; Abam et al. 1997).

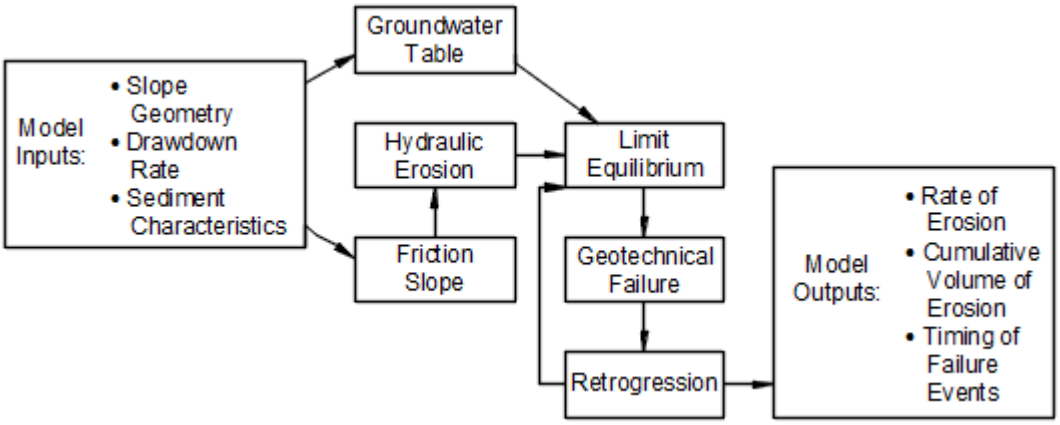


**Figure 1.** Model Workflow.

Model simulation begins with the input of slope geometry, which is defined with station-elevation points (henceforth "nodes") from left (channel thalweg) to right (bank crest). The duration of model simulation is defined by the number of time steps, where calculations are completed for each time step. There is a one-day warm-up period for the model with the starting water level before drawdown is initiated to ensure slope stability is independent of drawdown. The sequence of calculations and submodels then follow the order of Figure 1.

### *2.1.1. Groundwater Table*

The significance of groundwater location and behavior with regards to slope stability is well-documented (Reid, 1992; Doyle et al. 2003; Greimann and Huang, 2006). Despite this relationship, a dynamic groundwater level is not represented in current bank stability models. Typically, a hydrostatic groundwater level is assumed constant through the bank length (Langendoen and Thomas, 2001), in contrast to the delayed response and convex shape observed during drawdown operations (Zhan et al. 2006).

To develop a dynamically-changing groundwater table to include elements of groundwater lag and a drawdown gradient, several references were used for

development of this submodel (Ibrahim and Brutsaert,1965; Verman and Brutsaert, 1971; Singh et al., 1985). An empirical relationship and lookup table (Singh et al., 1985) were implemented as a submodel to predict groundwater levels in a slope based on the soil characteristics, bank length, initial groundwater height, and the time step of external drawdown (Figure 2).

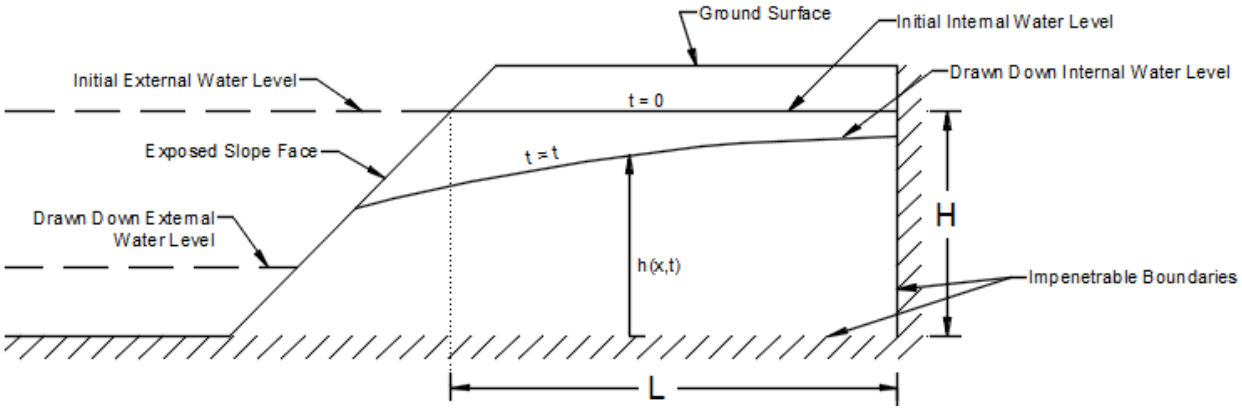


**Figure 2.** Conceptual diagram adapted from Ibrahim and Brutsaert (1965).

The groundwater head (h) was determined for any point (x) along the length of the bank at any time step (t). As the external water level is lowered during drawdown periods, a dimensionless time value was approximated based on the time elapsed and physical properties of the sediment (Eq. 1). Dimensionless time in this case is derived from Darcy's Law for flow of fluids through porous media (Ibrahim and Brutsaert, 1965).

$$T = \frac{kH}{S_y L^2} t \qquad \text{[Eqn. 1]}$$

Where T = dimensionless time (-), k = hydraulic conductivity (m/hr), H = initial horizontal water level of the free surface at t=0 (m), t = time (hr), $S_y$ = specific yield (-), and L = distance from the intersection of the external water level on the bank slope to the last point of the bank crest (m). Hydraulic conductivity and specific yield are set as values determined from the field, or typical values in the literature for the sediment type (Holtz et al. 2013; Domenico and Schwartz 1990). Based on dimensionless time and the distance along the bank with respect to the total bank length, empirical values for the dimensionless drawdown of groundwater were

established (Singh et al., 1985). Thus, the groundwater level is not a static, horizontal line through the slope, but was represented as a non-linear line.

### *2.1.2. Friction Slope*

The friction slope, defined as the slope of the energy grade line (Chaudhry, M.H. 2008) and represented as the longitudinal change in water surface elevations in reservoirs, is nearly zero. As the water level is drawn down, the friction slope is expected to increase as the water depth decreases and the surface tilts towards the outlet. In the early drawdown phases, entrainment of the toe will be practically negligible as the pool surface remains relatively flat. At some point during the drawdown, the friction slope will increase such that boundary shear stress overcomes the critical shear stress of the material at the toe, leading to hydraulic erosion of the toe.

To estimate the change in friction slope at any point longitudinally in the impoundment over the drawdown period, a subset of the standard step method was used (Chaudhry, M.H. 2008). This method assumes gradually varied flow under steady state conditions and starts computations at a location where the flow depth for the specified discharge is known.

$$S_e = \frac{n^2 q^2}{y_i^{(10/3)}} \qquad \textbf{[Eqn. 2]}$$

Where $S_e$ = friction slope of the water surface (m/m), n = Manning's roughness coefficient (0.05 $m^{1/3}/s$), q = unit discharge (0.167 $m^2/s$), and $y_i$ = water depth at time step "i". The Manning's roughness coefficient is appropriate for slow-moving, natural streams with deep pools (Chow, 1959). The unit discharge was estimated by taking the mean discharge reported in Randle et al. (2015) during each drawdown period and dividing by the cross sectional width. The friction slope was calculated for each drawdown increment, replacing the initial water depth with the lowered depth.

### *2.1.3. Hydraulic Erosion*

Erosion of the bank toe and channel bed can increase the height and angle of the bank up to the point that gravitational forces are greater than the shear strength of the bank material, initiating geotechnical failure (Simon et al 2000). The approach and equations applied herein are based on methodology described in Bankhead et al. (2013). The lateral hydraulic erosion distance (E) of each node of the bank geometry below the external water level can be calculated based on:

$$E = \varepsilon \Delta t \quad \textbf{[Eqn. 3]}$$

Where E = hydraulic erosion distance (m), ε = hydraulic erosion rate (m/hour), and Δt = time step (hour). The hydraulic erosion rate depends on the soil and channel characteristics to determine the stresses involved:

$$\varepsilon = K(\tau_o - \tau_c) \quad \textbf{[Eqn. 4]}$$

Where K = hydraulic erodibility coefficient, $\tau_o$ = boundary shear stress ($N/m^2$), and $\tau_c$ = critical shear stress ($N/m^2$). The critical shear stress as a function of D50 was derived from Berenbrock and Tranmer (2008). The erodibility coefficient and boundary shear stresses are calculated as:

$$K = 1.62 * 10^{-6} * {\tau_c}^{-0.838} \quad \textbf{[Eqn. 5]}$$

$$\tau_o = \gamma_w RS \quad \textbf{[Eqn. 6]}$$

Where $\gamma_w$ = unit weight of water ($kN/m^3$), R = hydraulic radius (m), and S = friction slope (m/m). The hydraulic radius is calculated as the vertical area between two discrete points on the slope geometry and the water surface. The friction slope is calculated as a function of unit discharge and water depth. At every time step, the erosion distance for every node of the bank below the water surface was calculated as a function of the friction slope and relative hydraulic radius.

### *2.1.4. Drawdown*

The two key variables driving sediment erosion during drawdown and decommissioning are the drawdown rate and the inflows during drawdown (Major et al., 2017). These two variables are often described as process-based erosion, in contrast with event-based erosion, where moderate and high flow events after drawdown shape the channel (Pizzuto 2002). This research emphasizes the first phase

(process-based erosion) due to drawdown, and thus the effects of reservoir inflows were not considered in this model. Especially when simulating impoundments with fine (sand, silt, clay) sediments, high discharges are not required to erode these sediments, in comparison to larger grains that need high-flow events to be transported (Pizzuto 2002).

### *2.1.5. Limit Equilibrium Method*

The limit equilibrium method is a commonly-applied approach for slope stability analysis in a two-dimensional space. The stability of a sliding soil mass is evaluated by comparing forces, moments, and stresses that resist and drive movement of the mass (Cheng et al., 2007; Figure 3). The output of this method is a factor of safety, (FS) or a ratio of the shear strength to the shear stress (Eqn. 7)(Bishop, 1955). A factor of safety less than 1.0 is considered unstable.

$$FS = \frac{\sum \frac{[c'b+(W-ub)tan\phi')}{cos\alpha(1+\frac{tan\alpha tan\phi'}{FS})}]}{\sum W sin\alpha} \quad \textbf{[Eqn. 7]}$$

The value of effective cohesion (c') is treated as undrained shear strength ($c_u$) based on typical values from the literature for undrained or drained conditions of the sediment type. The width of each slice (b) is the distance between each discrete node of the slope geometry. Weight of the slice (W) is calculated as the slice area multiplied by unit weight of the sediment type. Pore water pressure (u) is calculated as the hydrostatic pore pressure at the base of a slice. Inclination of the slice base (α) is calculated as the angle of the base along the failure surface. Effective friction angle (φ') is the internal friction between the bank grains, and is set based on values from the field, or typical values from the literature (Holtz et al. 2013; Domenico and Schwartz 1990) for undrained or drained conditions of the sediment type.

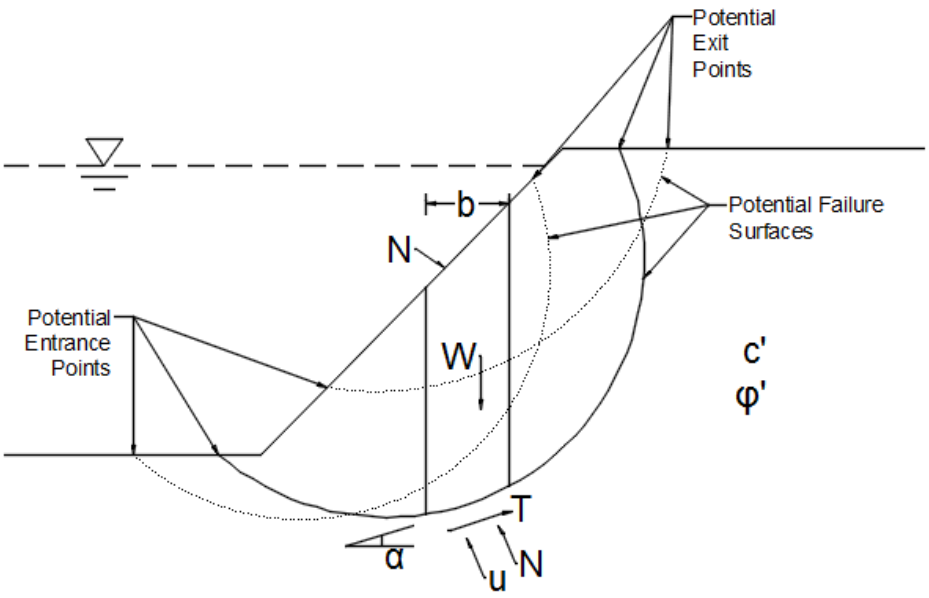


**Figure 3.** Illustration of Bishop's Method applied to a simplified slope with the variables from Eqn. 1 indicated. FS = factor of safety (-), c' = effective cohesion ($kN/m^2$), b = width of each slice (m), W = weight of the slice (kN/m), u = pore water pressure ($kN/m^2$), α = inclination of slice base (degrees), and φ' = effective friction angle (degrees).

### *2.1.6. Geotechnical Failure*

This model was developed to represent rotational failures, which are not included in common bank stability models (Cantelli et al., 2007), despite their importance for systems dominated by fines. Rotational failures generally occur in very high banks of homogeneous, fine-grained materials characterized by bank angles that are less than the angle of internal friction (φ') (Bankhead et al. 2013). To determine the slip surface for a given time step, the model evaluates thousands of potential surfaces by combining entrance and exit points with varying radii (i.e. a small radius gives a deep circular cut, whereas a long radius provides a near planar surface)(Figure 3).

The model's application of a Simplified Bishop's (Bishop, 1955) Method of Slices discretizes the soil mass into vertical blocks for force equilibrium calculations and determines moment equilibrium about the center of a circular slip surface. Horizontal forces are not considered for each slice, thus interslice shear forces are

zero. Instead, shear and normal stresses from failing blocks are applied to the surface of the next set of blocks and considered in their stability (see Section 2.1.7 and Figure 4 for details). The factor of safety is calculated iteratively based on Eq. 7. At the end of a time step, all failure surfaces with a factor of safety less than 1.0 are considered failed. The volume of sediment resting on the failure surface is immediately removed from the system without accumulation at the toe.

### *2.1.7. Retrogression*

Retrogression is a mechanism of bank failure due to initial failure of the slope that (a) removes support for the remaining sediment and (b) triggers a series of failures that move up-slope (Abam 1997). This process is well documented in dam removal case studies. Wilcox et al. (2014) noted that sequential shallow-seated failures and landsliding eroded 1/3rd of stored reservoir sediments in one week at the Condit Dam Removal. Doyle et al. (2003) observed deep-seated rotational slumping of reservoir banks due to base lowering during the removal of LaValle Dam. Despite the observation of retrogression in the field, this mechanism is not represented in current models of impoundment evolution.

Retrogression was modelled by applying the shear and normal stresses from the previous failing mass to the surface of the next set of blocks in evaluation of their stability. The downdrag (T) of the first failing block provides a driving force, versus the normal stress (N) of previous failures that provide a resisting force (Figure 4). The shear and normal force interactions between all failure blocks are evaluated until the slope is considered stable in order to capture all unstable surfaces within the same time step. These interacting forces between blocks are important when simulating the mechanisms that cause geotechnical failures of banks, especially in impoundments with an appreciable amount of silt and or clay (Haug et al. 1977).

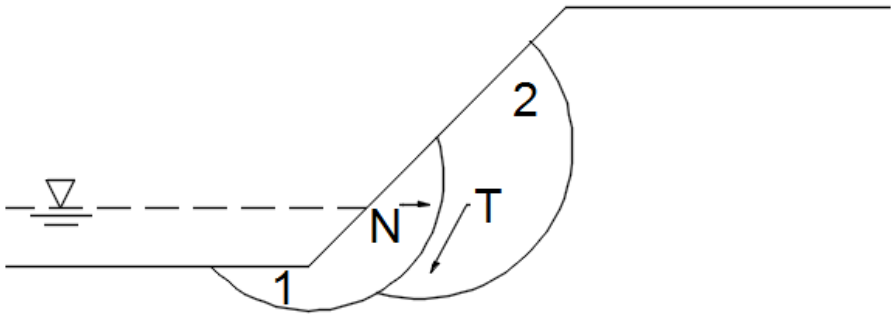


**Figure 4.** Retrogression of a slope after drawdown where block 1 is a rotational failure applying normal (N) and shear (T) stress to block 2, causing a second rotational failure.

## 2.2. Case Study

### *2.2.1. Background*

True validation of the model was not possible due to lack of high frequency surveys for reservoir drawdowns. Instead, field observations (Randle et al., 2015; Bountry et al., 2011) from the Elwha dam removal were used to provide a representative example of pre-drawdown reservoir geometry, soil characteristics, and drawdown rate in a reservoir. Elwha Dam (Figure 5(A)) was a 32 meter high concrete gravity dam that formed Lake Aldwell on the Elwha River in Washington before its removal, which began in 2011. To control the sediment release from this dam, the management plan called for staged removal over a two- to three-year period (Table 1). Pre-removal bathymetry, sediment sampling, and reservoir drawdown rates were measured during this removal process. The physical characteristics of the sediment used in this simulation was based on the fine-grained reservoir sediment of Lake Aldwell (Table 2).

### *2.2.2. Model Scenarios*

Two numerical experiments were simulated to examine the individual and synergistic effects of drawdown rate and grain size on the rate, magnitude, and timing of lateral erosion in a reservoir. Rate of erosion is calculated as the single minimum and maximum volumes of erosion that are generated by the entire bank during one time step. Magnitude of erosion is the cumulative volume of erosion from the entire simulation. Timing of erosion is the time step(s) at which erosion occurs.

**Evaluating the Effect of Drawdown Rate**

Five drawdown rates were simulated. Three staged drawdowns were simulated to evaluate the expectation that the rate of sediment evacuation varies with the phases of staged drawdown: one scenario represented that actual drawdown conducted during the removal of Elwha Dam (henceforth “Staged”), one scenario that shortened the drawdown phases with longer hold periods (henceforth “Staged-Short”), and one scenario that extended the drawdown phases with shorter hold periods (henceforth “Staged-Long”) (Table 1). The Staged-Short scenario was

designed so that the drawdown increment occurred more rapidly than the actual Staged scenario, with each increment occurring in one day and the remaining days of the stage filled by a hold period. The Staged-Long scenario was designed for an extended drawdown period, such that each hold period was shortened to one week and the reservoir was lowered the remaining days of the stage. A duration of one week for the hold periods falls within the typical range used in dam removals (Randle et al., 2017) and allows for a distinct separation between each increment of drawdown.

**Table 1.** Drawdown Scenarios for Lake Aldwell. Note that the total drawdown increment was the same (9m) for all drawdown scenarios.

| **Alternative** | **Drawdown Increments (m)** | **Drawdown Duration (days)** | **Hold Period (days)** |
|---|---|---|---|
| Staged | 4.3 | 9 | 112 |
| | 2.1 | 5 | 14 |
| | 2.6 | 1 | 42* |
| Staged-Short | 4.3 | 1 | 120 |
| | 2.1 | 1 | 18 |
| | 2.6 | 1 | 42 |
| Staged-Long | 4.3 | 114 | 7 |
| | 2.1 | 12 | 7 |
| | 2.6 | 36 | 7 |
| Slow | 9 | 183 | 0 |
| Rapid | 9 | 1 | 182 |

*Actual hold period went for 8 weeks, but was limited to the first day of December for this simulation due to rising inflows in the field setting.

The effect of slow drawdown on erosion rate and volume was represented by continuously lowering the water level the same amount (9 meters) over the same period (183 days), rather than in phases with hold periods. It is expected that Slow drawdown will decrease the volume and rate of lateral erosion relative to Rapid drawdown, with failures occurring later in the simulation. The effect of Rapid drawdown on erosion rate and volume was represented by a "worst case", or instantaneous, scenario, where the water surface is lowered 9 meters in one day followed by 182 days of no drawdown. Rapid drawdown is predicted to increase the volume and rate of lateral erosion, with failures occurring in the first time step of the simulation. All five scenarios were run with the same geometry and soil characteristics to isolate the effect of drawdown specifically.

**Evaluating the Effect of Grain Size**

To examine the role of grain size on erosion volume and rate, the same geometry and five drawdown scenarios from the last experiment were simulated with coarse-grained material. It is expected that a larger grain size will decrease the magnitude and rate of erosion relative to the fine-grained scenarios. The physical characteristics of this coarse material was based on the delta sediment of Lake Aldwell (Table 2).

### 2.2.3. Input Parameters

**Slope Geometry**

A digital elevation model (DEM) of Lake Aldwell (Randle et al., 2015) representing pre-drawdown geometry was developed from bathymetric and topographic survey data collected in July 2010, along with LIDAR data from 2009 and 2012. A cross section was extracted from this surface in ArcMap 10.5.1 (Figure 5(B)). This cross section was selected due to its relative proximity to the dam.

To prevent numerical instability in the slope stability analysis, several assumptions were made for the bank geometry. Since the model proceeds from left to right, the cross section was truncated at the thalweg to split the entire cross section into two separate bank slopes. For a single bank, the bank crest and toe were extrapolated an additional distance to allow room for the failure surfaces to find entrance and exit points without being limited by the input geometry. A thalweg (in the x-direction) with a length 1/10th of the total bank length is added before the first survey point to provide an initial surface for failures to occur below the toe of the bank. The extended bank crest simulates reality where the hillslope would continue, beyond the last survey point recorded, at a constant slope. Finally, the surveyed bank slopes from the case studies were smoothed so that each point monotonically increased to the next. A sensitivity analysis was completed with finer discretization of the geometry (approximately 2 meters between station points). There was no difference between failures calculated in this scenario or in the finer discretization scenario.

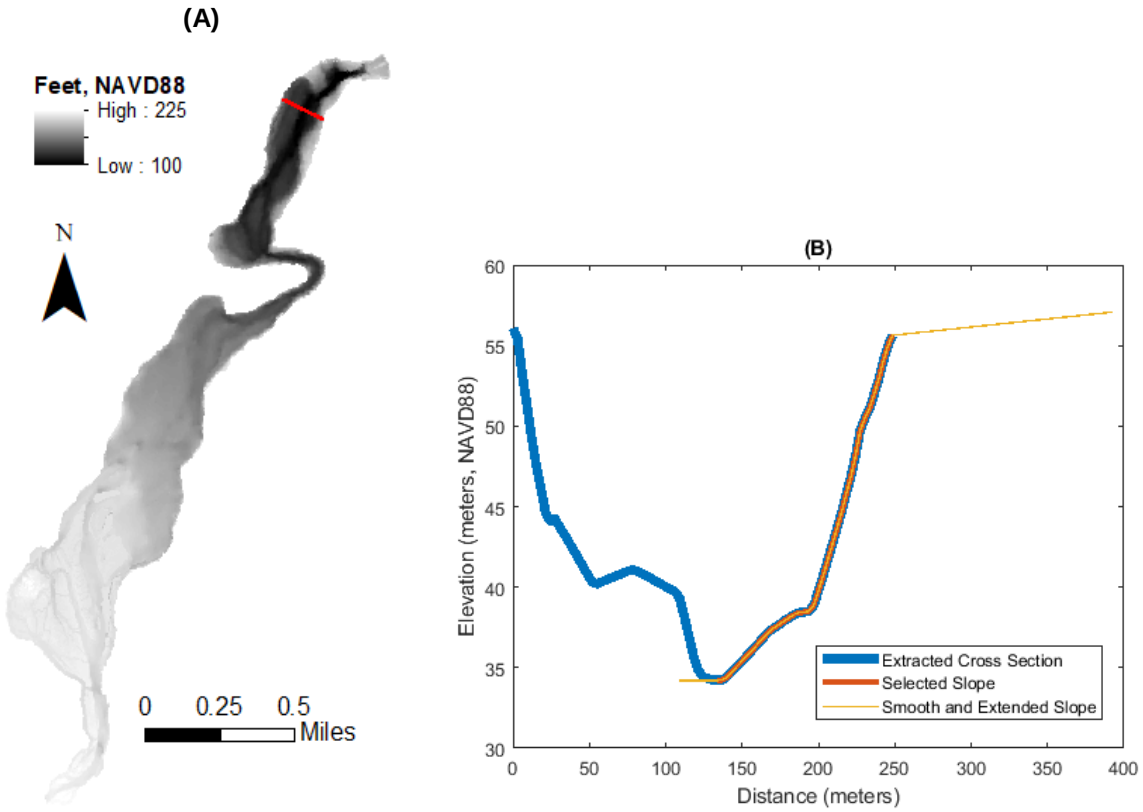


**Figure 5.** (A) Location of the selected cross section in Lake Aldwell and (B) extracted cross section geometry with chosen slope highlighted.

The average longitudinal channel slope in the reservoir was estimated to be 0.03 m/m using the pre-removal DEM. To prevent failure surfaces from passing through predam sediments, an impenetrable boundary was established relative to the input geometry. Assuming a non-erodible surface beneath the reservoir sediments helps represent how the predam topography is more resistant to erosion than the accumulated sediments at most reservoirs (Randle 2017). The impenetrable boundary was estimated to be 1.14 meters below a thalweg from a second DEM developed by USBR (Randle 2015), based on historical surveys and sediment thickness estimations. The initial water depth was set to 26.5 meters based on the water surface elevation at Lake Aldwell for the first date of drawdown (USBR Pacific Northwest Hydromet).

**Sediment Characteristics**

The sediment characteristics for D50s found in the Lake Aldwell reservoir and delta (Table 2 were estimated based on typical values found in the literature (Holtz et al. 2013; Domenico and Schwartz 1990). The reservoir bottom and hillslopes were reported to be almost entirely composed of silt and clay, versus the delta which contained medium sand at the cross section selected (Randle et al. 2015).

The following conditions were assumed for each drawdown scenario for fine material: undrained for short phases of drawdown (Rapid, Staged, and Staged-Short) and drained for long phases of drawdown (Slow, Staged-Long) and the hold periods for the staged scenarios. The drawdown scenarios for coarse material are assumed to be drained in all cases. Thus, the input parameters are different depending on sediment type and condition and may vary throughout a simulation.

**Table 2.** Summary of Sediment Characteristics and Associated Information.

| | **Lake Aldwell Cross Section** | | |
|---|---|---|---|
| | **Fines** | | **Coarse Material** |
| **Parameter** | **Undrained** | **Drained** | **Drained** |
| $D_{50}$ (mm) | 0.008 | | 0.6 |
| Effective Cohesion (kPa) | 0.1 | 0 | 0 |
| Undrained Shear Strength Gradient | 0.35 | 0 | 0 |
| Effective Internal Friction Angle (degrees) | 0.1 | 30 | 33 |
| Unit Weight ($kN/m^3$) | 14 | | 20 |
| Hydraulic Conductivity (m/day) | $9*10^{-6}$ | | 0.4 |
| Porosity (%) | 60 | | 50 |
| Specific Yield (%) | 3 | | 28 |

# 3. RESULTS

## 3.1. Model Verification

Numerical validation of the model was not possible due to a lack of high frequency reservoir surveys during reservoir drawdown. Instead, individual processes were qualitatively verified for expected behavior.

### *3.1.1. Hydraulic Erosion of the Toe*

Hydraulic toe erosion behaved as expected for all drawdown scenarios of fine-material (Figure 6). The hydraulic radius for this verification was calculated from the first discrete point of the slope geometry and was equivalent to water depth for the entire simulation. As water depth decreased, boundary shear stress increased due to the increase in friction slope of the water surface.

Although the critical shear stress for the fine material simulated was just 0.038 $N/m^2$, the boundary shear stress generated over the course of drawdown was not high enough to induce hydraulic erosion. The large width of the reservoir minimized the unit discharge, which was small relative to the water depth and reduced the friction slope. As water depth decreased, the unit discharge and friction slope increased, but not enough to generate excess shear stress as seen in this system and other reservoirs (Olsen and Haun, 2018).

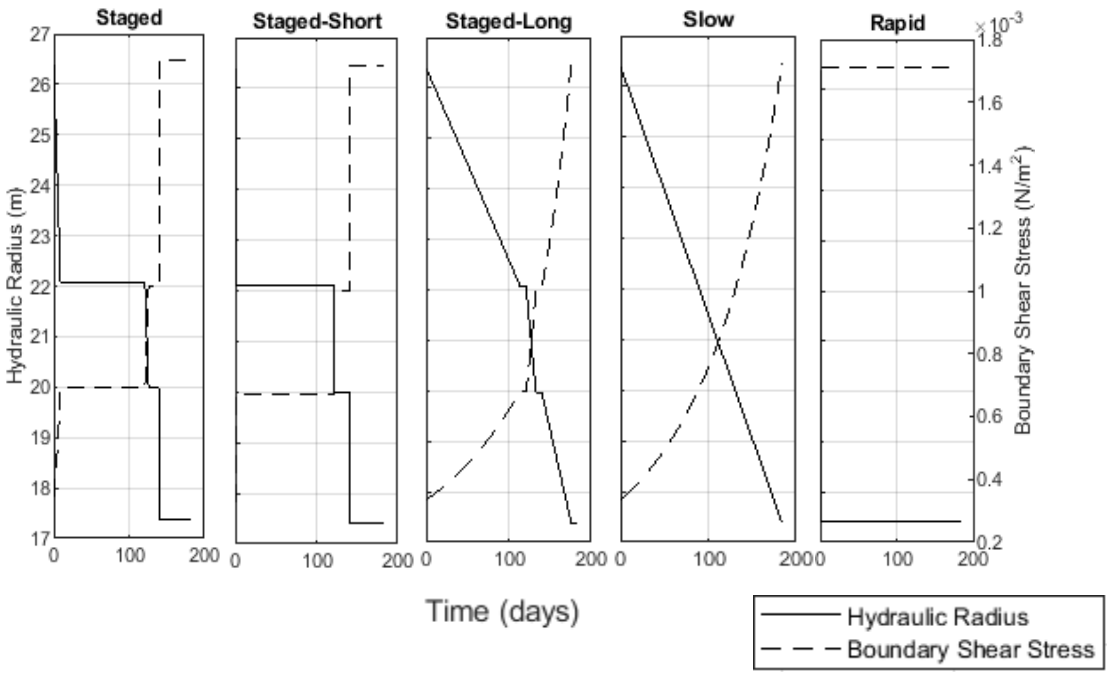


**Figure 6.** Comparison of parameters used to calculate hydraulic erosion for each fine-grained drawdown scenario. Critical shear stress of the fine material is 0.038 N/m$^2$.

### *3.1.2. Geotechnical Failure*

Results of the assessment of model behavior in producing geotechnical failure are presented for the Staged drawdown of fine-material (Figure 7), as it occurred at the Elwha Dam removal. The first failure block during retrogression had the lowest factor of safety, with stability increasing for each sequential failure within a single time step, as expected (Abam 1997). The weight of the failed blocks was lower for the first set of failed blocks than for the second set of failed blocks, which aligns with the magnitude of volume eroded at time. As initial failures increased the steepness of the slope, the mean slope of failure for sequential failures increased accordingly (Abam 1997). Retrogression of several failure surfaces within the same time step caused sequentially larger submerged depths as the surfaces progressed deeper into the bank (Chen and Huang, 2011). The submerged depth is the distance below the water surface at which the failure surface occurs. Geotechnical failure behaved as expected for all drawdown scenarios for fine and coarse grained materials (Appendix A).

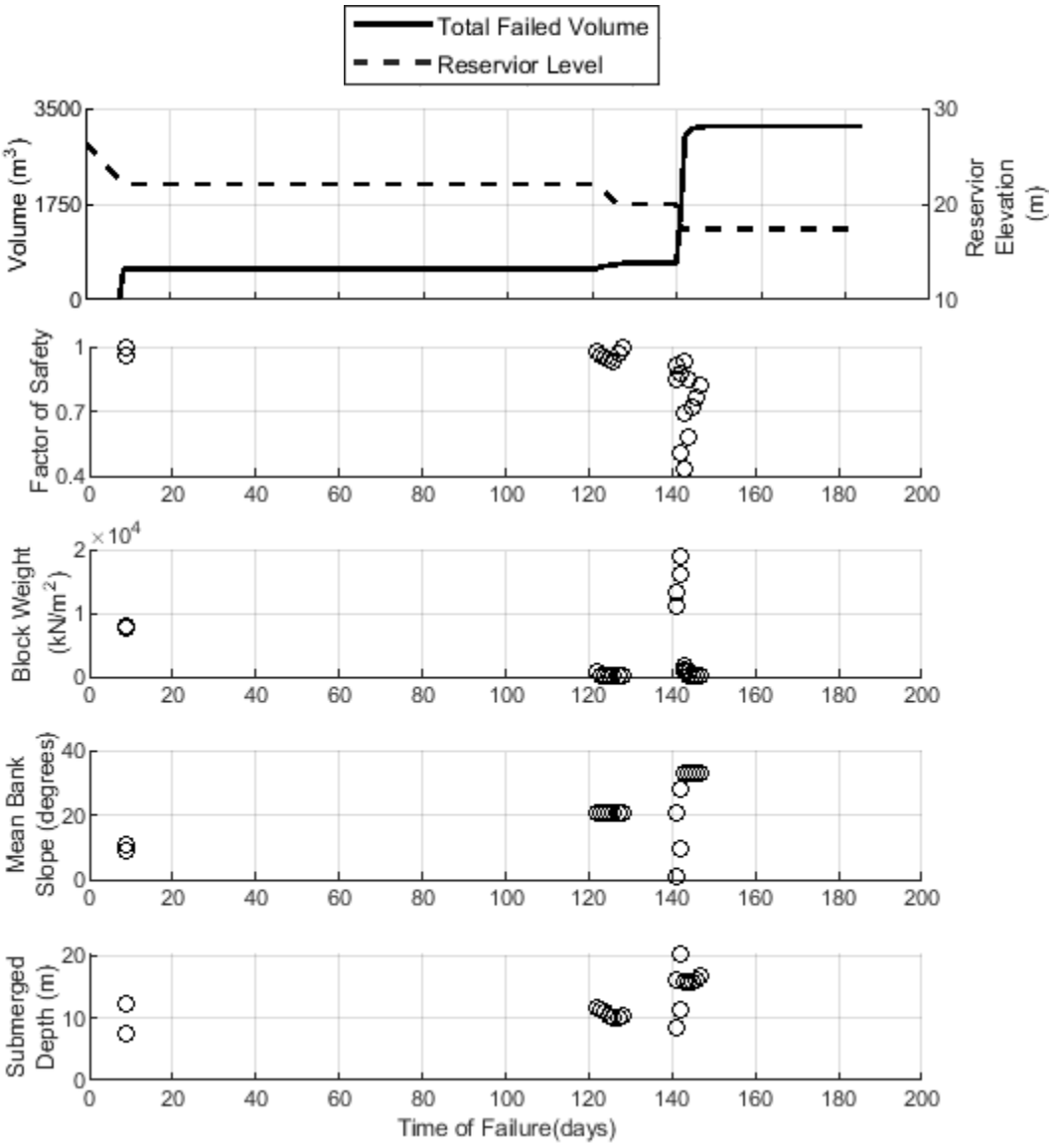


**Figure 7.** Comparison of parameters used to calculate geotechnical failure for the Lake Aldwell reservoir cross section during Staged drawdown.

## 3.2. Effects of Drawdown on Volumetric Rates of Erosion, Cumulative Volume of Erosion, and Timing of Erosion Events

Model results indicated that the Slow and Staged-Long scenarios did not produce any failures (Figure 8, Table 3). Slow and Staged-Long drawdown were very similar in design, due to the short hold periods for the Staged-Long scenario and small drawdown increments for the Slow scenario.

Contrary to the expectation that Rapid drawdown would produce the largest erosion rate in any given time step, the model results indicated that Staged and Staged-Short produced the largest erosion rates (Figure 8, Table 3). The Staged and Staged-Short drawdown scenarios produced the largest maximum rate of erosion, even though the scenario produced the smallest minimum rate of erosion. Rapid drawdown produced the largest minimum rate of erosion in any given time step. The minimum erosion rate represented the smallest volume of erosion produced in a single time step by small bank failures, compared with the maximum erosion rate, which generated the largest volume of erosion in a single time step with larger bank failures. The range in erosion rates is illustrated by the differences in erosion geometry between sequential failures (Figure 9) and the weight of failure blocks (Appendix A).

Model results confirmed the expectation that the Rapid drawdown scenario generated the largest cumulative volume of erosion across the entire drawdown period, though the differences in cumulative volumes between Rapid, Staged, and Staged-Short drawdowns were small (Figure 9, Table 3). The use of Staged drawdown with short drawdown durations (Staged-Short) produced the lowest cumulative erosion rate of the scenarios that produced bank failures.

Deeper drawdown increments that occur with faster lowering of the reservoir (Rapid, Staged-Short) generated failures earlier in the simulation than relatively smaller drawdown increments (Staged), even if they did not necessarily lead to larger cumulative erosion volumes. The Rapid drawdown scenario generated its entire volume of erosion after less than 2% of the total simulation time (Table 3). Rapid drawdown produced the largest cumulative volume of erosion over the smallest number of failures, producing more sediment per event. While Staged and Staged-

Short produced similar cumulative volumes of sediment to Rapid drawdown, the sediment was produced by many, mostly small events.

**Table 3.** Summary of results for the rate of erosion, cumulative volume of erosion, and timing of erosion from each drawdown scenario for fine-material.

| | **Staged** | **Staged-Short** | **Staged-Long** | **Slow** | **Rapid** |
|---|---|---|---|---|---|
| **Minimum Rate of Erosion ($m^3$/day)** | 10 | 11 | N/A | N/A | 1071 |
| **Maximum Rate of Erosion ($m^3$/day)** | 1357 | 1357 | N/A | N/A | 1199 |
| **Cumulative Volume of Erosion ($m^3$)** | 3171 | 3164 | 0 | 0 | 3465 |
| **Number of Failures** | 21 | 20 | 0 | 0 | 3 |
| **Timing of Failure Events (days)** | 9, 122-128, 141- 147 | 1, 122-125, 141-146 | N/A | N/A | 1-3 |

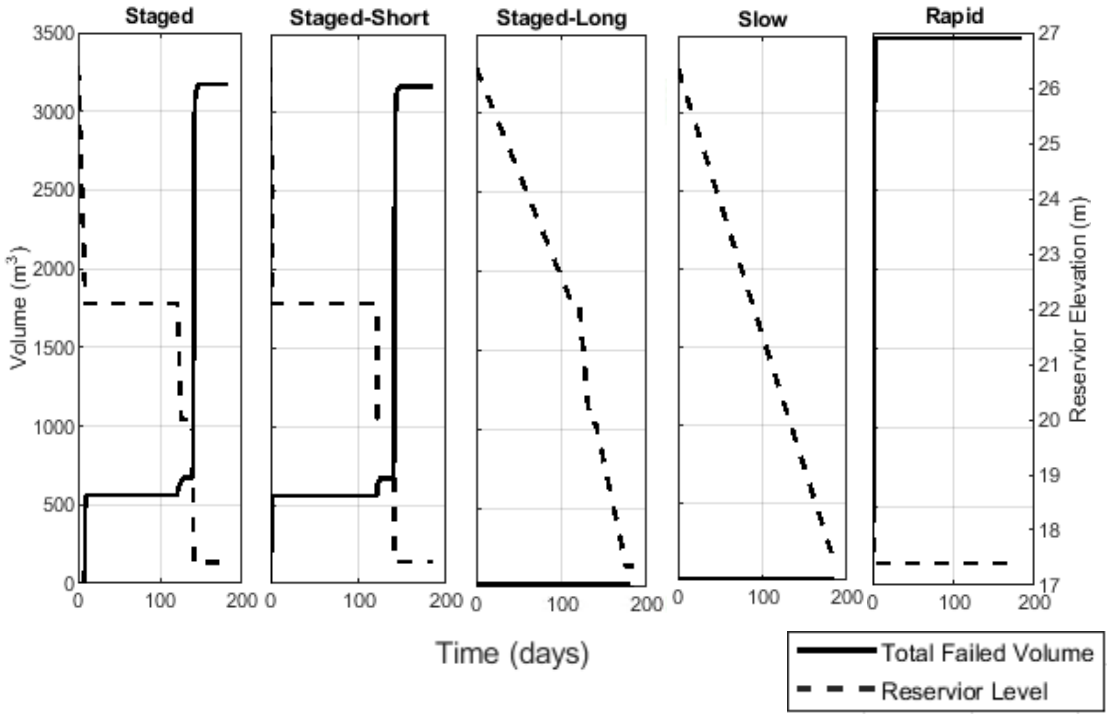


**Figure 8.** Comparison of erosion time series from each drawdown scenario for fine sediment.

Differences in failure geometry across drawdown scenarios illustrated how mechanisms driving failure varied with drawdown increments. Although the Rapid and Staged-Short scenarios had the largest drawdown increments, the differences in their erosion geometry demonstrated different mechanisms of erosion during the drawdown simulation. Short drawdown increments in the Staged-Short scenario generated rotational failures with smaller radii, with several failure surfaces occurring in the first block. In contrast, the Rapid scenario produced only three large rotational failure surfaces. With more failure surfaces, the Staged and Staged-Short scenarios reached a submerged depth of 20.3 meters compared to the Rapid scenario that reached just 18.5 meters. In addition, a transition from rotational to planar failures for Staged and Staged-Short drawdown occurred as erosion progressed into the bank. The mean angle of the progressive failures increased for Staged and Staged-Short as the failures became planar (Appendix A).

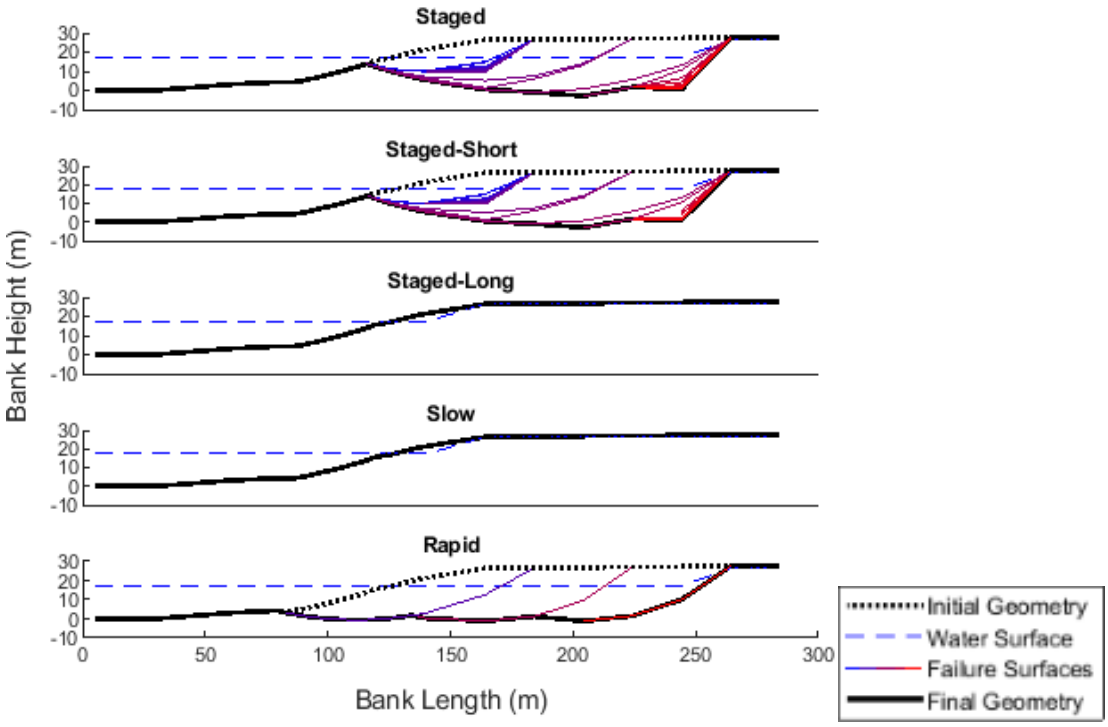


**Figure 9.** Comparison of erosion geometry from each scenario for fine material. The color of the failure surfaces indicate the sequence in which the failures occurred, starting with blue as the first failure, transitioning through purple, and ending with red for the last failure.

## 3.3. Effects of Grain Size on Volumetric Rates of Erosion, Cumulative Volume of Erosion, and Timing of Erosion Events

As expected, a larger grain size increased bank stability and reduced the magnitude and rate of erosion compared to fine-material (Figure 10). When replaced with sand-sized material, none of the five drawdown scenarios generated erosion. The fine-grained scenario had a friction angle of 30 degrees, compared to the coarse-grained scenario with a friction angle of 33 degrees. This difference in these values caused a 12% increase in the shear strength term for Equation 7, raising the resisting forces acting in the coarse-material bank.

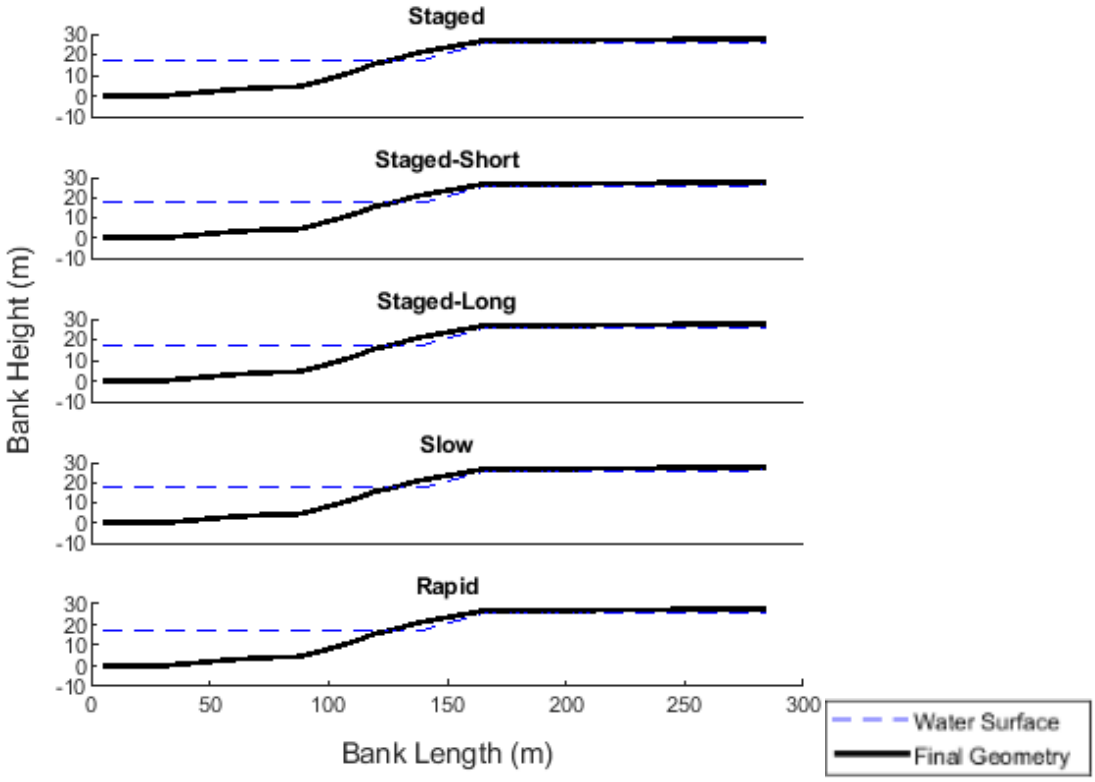


**Figure 10.** Comparison of erosion geometry from each scenario simulated for coarse material.

# 4. DISCUSSION

## 4.1. Mechanisms of Erosion

Model results identified important patterns in how drawdown rate and grain size interact to produce different erosional sequences and volumes. These patterns support interpretations of different mechanisms producing bank failure and lateral erosion during Rapid drawdown of reservoirs. During Rapid drawdown, ponding water acted as a buttress, effectively stabilizing the slope during rapid changes in stress and the associated onset of undrained loading conditions. As ponding water on the slope face was lowered, so were stabilizing hydrostatic pressures, leaving the bank in an undrained state and more susceptible to failure (Maihemuti et al., 2015). Under rapid drawdown conditions, we assumed that significant changes in external ponding resulted in mobilization of only undrained shear strength, $c_u$, (i.e. $\varphi' = 0°$ conditions) consistent with the observed loading response of saturated, fine-grained

materials. A lack of mobilized internal friction in an undrained state simplified Equation 7 such that undrained shear strength was the major resisting force and block weight the major driving force. For the given parameters, the undrained shear strength was insufficient to keep the slope stable after buttressing forces from ponding water were removed, resulting in the sequence of large critical failure surfaces seen in the failure geometry for Rapid drawdown (Figure 9).

In comparison, no erosion stemming from bank failures occurred during Slow and Staged-Long drawdown scenarios under the drained conditions produced by the slow loss of buttressing water. While the stability of streambanks under drained conditions are typically controlled by friction angle and pore water pressure (Stark et al., 2005), friction angle governed shear strength under these model scenarios under the working assumption of stress changes that are sufficiently slow as to not generate excess pore pressures. Slow drawdown of the reservoir was associated with drained conditions for the bank, which allowed fine sediment to retain its shear strength due to the internal friction between grains (Duncan et al., 2014). In slope stability, the presence of internal friction increases the factor of safety and decreases the slip body volume and slip surface depth, even in silty soil (Lin et al., 2013). The slow loss of buttressing water allowed the saturated bank, under drained conditions, to stay in place, such that the resisting internal friction overcame the weight of the bank as a driving force.

Staged drawdowns can produce a range of erosion volumes depending on how long the drawdown phases are relative to the hold periods. The fast drawdown phases for Staged-Short was associated with undrained conditions that produced multiple failures. In contrast, a stable but saturated bank was produced in the case of Slow and Staged-Long drawdown. The modeled stability of the Staged-Long scenario results reflected the goals of the staged drawdown for the Elwha Dam removal, which focused on minimizing the drawdown increment to prevent deep-seated failures along the reservoir shoreline (Bountry et al. 2018, Czuba et al., 2011). However, the importance of hold periods was more clearly seen in the Staged and Staged-Short scenarios, where less than one-third of failures occurred outside of the drawdown increments. Hold periods were simulated as drained conditions such that slope

stability was high, due to the presence of internal friction, in comparison to the undrained conditions of drawdown increments. The hold periods can be critical in reducing the quantity of sediment eroded from the reservoir (Doyle et al., 2003) and the rate of sediment release (Cantelli et al., 2004). We note that the model results contrast with observations from the Elwha Dam removal, where hold periods induced lateral erosion stemming from channel avulsion and meandering (Randle et al., 2015). However, the high flow conditions and channel migration that occurred in Lake Aldwell to drive lateral erosion in the delta were not represented in this model.

As expected, the timing of erosion was directly related to the drawdown design, with erosion occurring earlier with Rapid drawdown and during drawdown increments for Staged drawdowns. This component of reservoir erosion is particularly relevant to sediment management, as the timing of sediment release can determine the degree of impact to downstream water quality, channel geomorphology, flooding potential, and habitat productivity (Czuba et al., 2011). The Condit Dam was instantaneously removed to decrease the time needed for the downstream reach to return to normal levels of suspended sediment (Magirl et al., 2010). In comparison, the Elwha Dam removal utilized hold periods to limit the amount of reservoir sediment released downstream during critical fish migration periods (Randle and Bountry, 2017). Not only was it important to reduce the maximum rate of erosion at any time for Elwha, but the management plan also aimed to raise the minimum rate of erosion to avoid affecting too many age classes of fish and prevent unstable sediment from remaining in the reservoir after dam removal (Bountry et al., 2018).

The results from this model illustrated a tradeoff between controlling how much impact is produced versus when the impact is produced for lateral erosion stemming from slope instability. Given the similarity between the cumulative volume of erosion generated by Staged, Staged-Short and Rapid drawdown, reservoir managers can base their design around the decision to have this volume released over a short or long period of time. The model results indicated that Staged drawdown can be designed through manipulation of the drawdown increments and hold periods to reduce the cumulative volume of erosion and volumetric rate of erosion. The Staged-Short scenario illustrated how relatively larger drawdown increments can remove

unstable sediment without generating the largest rate of erosion. The hold periods represent windows of time where erosion can be greatly reduced or eliminated following the drawdown increments. The duration of hold periods was less important than the duration for each depth increment in the drawdown, since the drawdown increment drove slope instability by producing undrained conditions. The physical, ecological, and societal goals of a dam removal or drawdown project can be used to dictate which scenario is best fit to achieve desirable outcomes.

The importance of effective internal friction angle was illustrated by the differences between the fine material to coarse material scenarios, as it produced a stable bank for all coarse grained scenarios. Bank stability typically decreases, and potential failure volume increases, as the bank slope angle approaches the effective friction angle of the sediment (Krahn et al., 1989; Cheng et al. 2006). Since the effective friction angle of the sand material (33 degrees) was sufficiently large in comparison to the maximum inclination of the bank slope (11 degrees), the model simulation behaved as expected; that is, no failures were observed under drained conditions. Although the unit weight of the sediment increased from fine to coarse material, consideration of mobilized internal friction considers overburden stress as both a resisting and driving force for factor of safety. The difference in results for fine- and coarse-grained scenarios is vital for reservoirs that contain spatially-variable deposits of sediment. Design of the drawdown strategy is not a “one-size-fits-all” approach in systems with spatially-varied stratigraphy, as the impact of drawdown increments and timing will vary throughout a reservoir depending on the stratigraphy.

This work highlights the importance of considering whether drawdown strategy will produce undrained or drained conditions, and which strength parameters may be present in those scenarios. Some dam removals are designed to rapidly flush fine sediments from the reservoir to minimize the duration of impact (Wilcox et al. 2014, State Water Resources Control Board 2018). As illustrated in the Rapid drawdown scenarios presented herein, this rapid unloading led to a scenario where undrained shear strength was the only term acting as a resisting force and was inadequate at maintaining a stable bank. On the other hand, drained sediments can be stabilized by friction between grains (i.e. internal friction angle) and apparent

cohesion, depending on saturation conditions. For the Slow drawdown scenarios presented herein, friction between grains was the only stabilizing force because soils were saturated. Hydraulic conductivities of the fine sediments were low, producing a slow drawdown of the groundwater table relative to the drawdown of the reservoir elevation, which left soils saturated. Thus, while apparent cohesion associated with negative pore pressures (i.e. matric suction) can produce very stable banks in unsaturated streambanks (Rinaldi and Casagli 1999), apparent cohesion was considered to be zero in all model simulations because soils remained saturated and the region above the groundwater table was sufficiently small with respect to saturated height. We speculate that the slow erosion rates observed at some dam removals with fine sediments (Kosky, et al., 2004; Randle et al., 2015; Doyle et al., 2003; Greene et al., 2013, Tullos et al., 2016; Foley et al., 2017) are associated with higher hydraulic conductivities relative to the drawdown rates that produced unsaturated conditions. However, the stabilizing effect of establishing drained conditions, even in saturated soils, is illustrated by the design of staged drawdowns of fine-grained reservoirs at Elwha, Glines Canyon, and Brewster Dam in an attempt to reduce the magnitude and/or rate of erosion (Major et al., 2017)

The inclusion of retrogression as an avenue for sequential block failures proved to be an important contribution as all fine-grained scenarios exhibited at least one time step with more than one failure. Although the block weight decreased with sequential failures in an individual time step, these additional failures added to the rate and cumulative volume of erosion that occurred during drawdown (Figure 7; Appendix A). For Staged and Staged-Short drawdown, six and 15 failures, respectively, occurred in a single time step with more than one failure. The sequential rotational failures that generated mass wasting for the fine grain scenarios was expected for banks with low slopes and cohesive material (Doyle et al., 2003).

In comparison, the dynamic groundwater submodel appeared to be less important for the fine-grained scenarios, given that the hydraulic conductivity of the sediment was four magnitudes less than the smallest drawdown increment. For the coarse material scenarios, the internal water level is more clearly drawn down towards the external water level due to the increased hydraulic conductivity, and may

have enabled sufficient mobilization of frictional shear strength under effective stress conditions. Reduced drawdown rates, relative to hydraulic conductivity, are expected to increase the importance of the dynamic groundwater submodel as it would provide an opportunity for unsaturated conditions to develop, and thus apparent cohesion to increase the stability of banks with fine material.

## 4.2. Limitations of the Model

Several aspects of lateral erosion were simplified or not included in this model. Entrainment of failed materials from the bank toe is one component that may help improve the accuracy of lateral erosion predictions, as failed materials are assumed to immediately leave the system in this model without accumulating at the toe. The incorporation of failed materials may reduce the magnitude or rate of erosion as it protects the slope sediment at the toe and would decrease the angle of the lower section of the slope as it accumulates (Lai and Wu, 2013).

Woody debris and vegetation are not considered in this model, though they influence the erosional processes in some reservoirs (Abam, 1997). For example, in Lake Aldwell, tree stumps in the reservoir sediment decreased the extent and rate of erosion by altering flow patterns and increasing the shear strength of the bank (Randle et al. 2017; Pearson et al. 2011). The inclusion of vegetation is expected to reduce the magnitude or rate of erosion as it adds shear strength to the bank sediments for additional resistive forces in the bank stability analysis (Bankhead et al., 2013).

The sediment in this model is assumed to be homogeneous, despite the complex facies architecture of the case study (Stratton and Grant, 2010) and some other reservoirs (Baker et al., 2018; Huang et al., 2019). Heterogeneous sediment can be simulated in some bank erosion models (Bankhead et al., 2013), although those models rely on planar failures through the layers of sediment. To reduce the difficulty of modeling circular failures through mixtures of coarse and fine sediment, assuming a representative, homogeneous sediment type was necessary. Depending on the mix of sediment types, the magnitude and rate of lateral may change. For example, a layer of fine sediment in the middle of a coarse material bank would provide a potential

failure surface with reduced shear strength that may cause geotechnical failure which would not ordinarily occur without the fine sediment (Stark et al., 2005).

The drained and undrained conditions were assumed for each scenario, where the sediment was drained during Slow and Staged-Long drawdown and hold periods, and undrained during Staged and Rapid drawdown. In reality, the transition between being undrained and drained is a function of pore pressure dissipation. This transition is much more complex than the model's approach to drained conditions being “on” or “off” based on the drawdown assumptions. Modeling the dissipation of pore pressures would be difficult based on transient hydraulic boundary conditions and the response of the sediment to loading (Duncan et al., 2014). Inclusion of this transition period may alter results, since undrained conditions were found to induce failure in the scenarios modeled. For example, adding a transition period to the Staged-Short scenario may result in the sediment functioning in an undrained state after the drawdown phases, rather than immediately switching to drained conditions, which would increase the potential for failures to occur.

While the focus of this model was on geotechnical failures that lead to lateral erosion, the decoupling of incision and lateral erosion in this model prevents these results from being expressed as a generalizable outcome for all dam removals. The relationship between incision and widening creates erosional sequences that define reservoir evolution from drawdown (Major et al., 2017). Conceptual channel-evolution models have been used for decades to describe channel development as a multistage, spatial and temporal sequence (Doyle et al., 2002). In reservoirs filled with sediment, the base-level fall from drawdown drains the impounded water such that incision creates a narrow channel that typically stops incising when the pre-dam gradient is achieved (Tullos et al., 2016). Through this process, the surrounding channel banks become over-steepened to promote lateral channel migration and mass movements (Major et al., 2012; Wilcox et al., 2014). As lateral erosion adds failed sediments to the incised channel, aggradation promotes further incision followed by widening again in a positive feedback look. Although a commonly coupled process in reservoir evolution, especially in deltaic sediments, incision is not relevant for the simulations in this paper as the water level was not lowered enough to expose

channel-bed sediments. Therefore, the results are focused solely on the direct impact of drawdown on exposed bank slopes through lateral erosion processes. There are linked bed and bank evolution models (Cantelli et al., 2007; Lai and Wu, 2013) that set the foundation in replicating the conceptual channel-evolution model through numerical modeling, with room for improving specific features (e.g. rotational failures, retrogression, groundwater).

As noted in model development, the representation of inflows that cause event-based erosion is not included in this model. Since this is not a hydrodynamic model, hydrographs cannot be used as inputs to generate a time-varying water depth relative to the channel geometry. Thus, this model is expected to only represent the process-based (sensu Pizzuto 2002) widening associated with drawdown. High storm flows after initial drawdown can be especially important in transporting additional reservoir sediment (Foley et al., 2017), as observed for the Merrimack Village and Simpkins dams (Collins et al., 2017). Incorporating the lateral erosion model proposed by this research into an existing hydrodynamic model may enhance the accuracy of predicting lateral erosion timing, rates, and magnitudes, especially in fine-grained, cohesive material. More current research has illustrated the ability to couple complex lateral erosion algorithms into 3-Dimensional adaptive water and sediment grids (Olsen and Haun, 2018).

## 4.3. High frequency surveys needed to study dynamic reservoir processes

The lack of high-frequency surveys throughout reservoir drawdowns inhibits detailed understanding of the sediment phenomena triggered by different drawdown scenarios. This model was developed in part to help examine the relevant processes, but is limited in the lack of verification data.

This is not an unusual obstacle for calibrating erosion models - from 2012 to 2017, there were less than 20 published studies on the physical or ecological river response to dam removal (Randle et al. 2017). Especially as 94% of removed dams have been less than 10 meters tall with less than 10,000 $m^3$ of accumulated sediment (Major et al., 2017), the physical effects of removing large dams are less well known.

Therefore, numerical modeling and scientific understanding could be improved if drawdown experiments and dam removals emphasize bathymetry surveys during the entire drawdown process.

For more focused efforts towards monitoring lateral erosion, periodic surveying of cross sections spatially representative of the reservoir are crucial. To isolate the impact of drawdown exclusively on slope stability without the influence of post-drawdown hydrology, high-temporal-frequency surveys during the drawdown process would be required. For example, the timing of surveys during staged drawdown could occur on the days that the drawdown phase starts and ends to see the direct influence of drawdown versus holding the water level. Coupling boat-based surveys of bathymetry (i.e. ADCP, sonar) with Unmanned Aerial Vehicle (UAV) flights can produce a powerful dataset for evaluating sediment phenomena with drawdown. UAV surveys allow for continuous imagery collection such that Structure-From-Motion (SfM) analyses can derive topographic point clouds (Baker et al., 2018). Although SfM cannot currently be used to accurately estimate underwater bathymetry, the frequent mapping of boundaries can be utilized to estimate rates of bank retreat. Combination of SfM surfaces with pre- and post-drawdown bathymetry surveys can be interpolated to estimate the volume of sediment eroded. Rigorous experimental design is a key component of collecting quantitative, reliable results from dam removals and drawdown experiments (Kibler et al., 2010).

Future work on this model could look towards its application and validation at other sites to better understand its strengths and limitations. Full integration into a hydrodynamic model would provide the opportunity to extend the duration of drawdown into periods that experience high flow events such that process- versus event-based erosion could be better understood. As dam height, reservoir size, and sediment grain size are crucial controls on erosional outcomes (Foley et al., 2017) the application of this model to other sites with various characteristics may generate a variety of results to better illustrate how all of these components are related.

# 5. CONCLUSIONS

Drawdown operations provide a missed opportunity to address concerns around sedimentation of reservoirs, controlling the outcomes of dam maintenance and removal, providing downstream fish passage, and mitigating the effects of sediment starvation downstream of dams. Understanding the geomorphic response of a reservoir during drawdown can have many benefits, such as minimizing the overall efforts of stabilizing the sediment while maximizing potential long term stability of the restored area (Doyle et al. 2002), or allowing for adaptive management to ensure that downstream sediment impacts are mitigated to acceptable levels (Randle et al., 2017). Confidence in predictive models can also be a powerful tool when communicating outcomes of drawdown with stakeholders, where public perception of project success can be critical for support (Tullos et al. 2016).

A numerical model was developed and simulated to examine how drawdown rate and grain size affect the rate, magnitude, and timing of lateral erosion in a reservoir. The drawdown of Lake Aldwell on the Elwha River in WA provided slope, geometry, sediment characteristics, and drawdown characteristics for the model. A novel groundwater submodel created a dynamic internal water level for improved bank stability analyses. Hydraulic erosion and geotechnical failure were calculated as the two processes that induce lateral erosion. The potential for sequential failures as retrogression was included as an additional component of the slope stability analysis. To evaluate the influence of drawdown on lateral erosion, the following scenarios were simulated: Staged, Staged with Short drawdown increments, Staged with Long drawdown increments, Slow, and Rapid drawdown. These scenarios were then re-evaluated with coarse material to understand the integrated impact of grain size and drawdown process.

Three overarching effects of drawdown emerged from the numerical experiments: 1) Staged drawdowns can produce a range of erosion volumes depending on how long the drawdown phases are relative to the hold periods, dictating the generation of undrained or drained conditions; 2) the timing of erosion was directly related to the drawdown rate, creating a tradeoff between the amount of impact created and when the impact is produced; and 3) coarse material reduces the

magnitude of erosion compared to fine material when the internal friction angle is greater than the bank slope angle. The inclusion of retrogression as an avenue for sequential block failures proved to be an important contribution as all fine-grained scenarios exhibited at least one time step with more than one failure. The duration of hold periods was found to be less important than the duration of drawdown increments, as the drawdown increment drives slope stability (e.g. undrained/drained conditions). As a majority of failures occurred under undrained conditions where undrained shear strength is present, the slope stability achieved under drained conditions highlights the importance of effective internal friction.

Several aspects of lateral erosion were simplified or not included in this model. These aspects include the immediate transport of failed materials, no incorporation of vegetation, homogeneous bank sediment, de-coupled incision and widening, assumed drained and undrained conditions, and a limit of model simulation to pre-high flow events. In addition, no validation data was available to check the accuracy of model predictions. The use of high-frequency bathymetry surveys or estimations of bank retreat through UAV surveys could be used to better understand the processes behind lateral erosion with quantitative pre- and post-drawdown data.

Further work with this model could focus on its integration into an existing morphodynamic model to couple these geotechnical bank stability algorithms with those that represent knickpoint migration and incision due to flood flows. Due to the complexity of sediment transport both spatially and temporally, comprehensive models of both fluvial and geotechnical processes are crucial in understanding the interconnected impact of drawdown operations.

# BIBLIOGRAPHY


1. Abam, T. K. S. (1997). Aspects of alluvial river bank recession: some examples from the Niger delta. *Environmental Geology*, *31*(3-4), 211-220.
2. Akbarizadeh, M., Saffarian, M. R., & Ghomeshi, M. (2020). Experimental investigation of sediment accumulation reduction in reservoirs due to turbidity currents with channel insertion at the entrance. *International Journal of Civil Engineering*, *18*(1), 37-47.
3. Baker, M. E., Miller, A. J., Van Ryswick, S., Boyd, E., Cashman, M. J., Collins, M. J., & Andrews, M. (2018, December). Tracking Geomorphic Change and Downstream Progress of Sediment Released by Removal of Bloede Dam, Lower Patapsco River, Maryland. In *AGU Fall Meeting Abstracts*.
4. Bankhead, N., Klimetz, L., Simon, A. (2013). BSTEM-Dynamic USER MANUAL.
5. Berenbrock, C., & Tranmer, A. W. (2008). *Simulation of flow, sediment transport, and sediment mobility of the lower Coeur d'Alene River, Idaho* (Vol. 5093). Reston, VA: US Geological Survey.
6. Bernander, S., Gustås, H., & Olofsson, J. (1989). Improved model for progressive failure analysis of slope stability. In *International Conference on Soil Mechanics and Foundation Engineering: 13/08/1989-18/08/1989* (Vol. 21, pp. 1539-1542). Balkema Publishers, AA/Taylor & Francis The Netherlands.
7. Bishop, A.W., (1955), "The Use of the Slip Circle in the Stability Analysis of Slopes", Geotechnique, Vol. 5, 7 - 17.
8. Bountry, J., Ferrari, R., Wille, K., & Randle, T. J. (2011). 2010 Survey Report for Lake Mills and Lake Aldwell on the Elwha River, Washington. In *US Bureau of Reclamation Technical Report No. SRH-2010-23*.
9. Bountry, J., Randle, T. J., & Ritchie, A. (2018). Adaptive Sediment Management Program Final Report for the Elwha River Restoration Project.
10. Bromley, C. (2008). *The morphodynamics of sediment movement through a reservoir during dam removal* (Doctoral dissertation, University of Nottingham).
11. Bureau of Reclamation. Pacific Northwest Region. Retrieved from https://www.usbr.gov/pn/hydromet/
12. Burroughs, B. A., Hayes, D. B., Klomp, K. D., Hansen, J. F., & Mistak, J. (2009). Effects of Stronach dam removal on fluvial geomorphology in the Pine River, Michigan, United States. *Geomorphology*, *110*(3-4), 96-107.
13. Cantelli, A., Paola, C., & Parker, G. (2004). Experiments on upstream-migrating erosional narrowing and widening of an incisional channel caused by dam removal. *Water Resources Research*, *40*(3).
14. Cantelli, A., Wong, M., Parker, G., & Paola, C. (2007). Numerical model linking bed and bank evolution of incisional channel created by dam removal. *Water Resources Research*, *43*(7).
15. Cetin, H., & Gökoğlu, A. (2013). Soil structure changes during drained and undrained triaxial shear of a clayey soil. *Soils and foundations*, *53*(5), 628-638.
16. Chaudhry, M.H. (2008). *Open-Channel Flow*. New York: Springer.

17. Chen, X., & Huang, J. (2011). Stability analysis of bank slope under conditions of reservoir impounding and rapid drawdown. *Journal of Rock Mechanics and Geotechnical Engineering*, *3*, 429-437.
18. Chow, V.T. (1959). Open-channel hydraulics: New York, McGraw-Hill, 680.
19. Crosa, G., Castelli, E., Gentili, G., & Espa, P. (2010). Effects of suspended sediments from reservoir flushing on fish and macroinvertebrates in an alpine stream. *Aquatic Sciences*, *72*(1), 85.
20. Cui, Y., & Wilcox, A. (2008). Development and application of numerical models of sediment transport associated with dam removal. *Chapter*, *23*, 995-1020.
21. Czuba, C. R., Randle, T. J., Bountry, J. A., Magirl, C. S., Czuba, J. A., Curran, C. A., & Konrad, C. P. (2011). *Anticipated sediment delivery to the lower Elwha River during and following dam removal*. US Department of the Interior, US Geological Survey.
22. Darby, S. E., Rinaldi, M., & Dapporto, S. (2007). Coupled simulations of fluvial erosion and mass wasting for cohesive river banks. Journal of Geophysical Research: Earth Surface, 112(F3).
23. Davis, C. M., Bahner, C., Eidson, D., & Gibson, S. (2014). Understanding reservoir sedimentation along the Rio Grande: A case study from Cochiti Dam. In *World Environmental and Water Resources Congress 2014* (pp. 2347-2357).
24. Domenico, P. A., & Schwartz, F. W. (1990). *Physical and chemical hydrogeology*. New York: Wiley.
25. Doyle, M. W., Stanley, E. H., & Harbor, J. M. (2002). GEOMORPHIC ANALOGIES FOR ASSESSING PROBABLE CHANNEL RESPONSE TO DAM REMOVAL 1. *JAWRA Journal of the American Water Resources Association*, *38*(6), 1567-1579.
26. Doyle, M. W., Stanley, E. H., Selle, A. R., Stofleth, J. M., & Harbor, J. M. (2003). Predicting the depth of erosion in reservoirs following dam removal using bank stability analysis. International Journal of Sediment Research, 18(2), 115-121.
27. Duncan, J. M., Wright, S. G., & Brandon, T. L. (2014). *Soil strength and slope stability*. John Wiley & Sons.
28. Epstein, JA 2009. Upstream geomorphic response to dam removal: The Blackfoot River, Montana. MS thesis, University of Montana.
29. Espa, P., Brignoli, M. L., Crosa, G., Gentili, G., & Quadroni, S. (2016). Controlled sediment flushing at the Cancano Reservoir (Italian Alps): management of the operation and downstream environmental impact. *Journal of environmental management*, *182*, 1-12.
30. Fan, J., & Morris, G. L. (1992). Reservoir sedimentation. II: Reservoir desiltation and long-term storage capacity. *Journal of Hydraulic Engineering*, *118*(3), 370-384.
31. Foley, M. M., Bellmore, J. R., O'Connor, J. E., Duda, J. J., East, A. E., Grant, G. E., ... & Craig, L. S. (2017). Dam removal: Listening in. *Water Resources Research*, *53*(7), 5229-5246.
32. Gibson, S., & Boyd, P. (2016). Monitoring, measuring, and modeling a reservoir flush on the Niobrara River in the Sandhills of Nebraska.

33. Greene, S. L., Krause, A. J., & Knox, J. C. (2013). A decade of geomorphic and hydraulic response to the La Valle Dam Project, Baraboo River, Wisconsin. *JAWRA Journal of the American Water Resources Association*, *49*(6), 1473-1484.
34. Greimann, B. P., & Huang, J. (2006). One-dimensional modeling of incision through reservoir deposits. In Hydraulic Engineers, Sedimentation and River Hydraulics Group, Technical Service Center, USBureau of Reclamation.
35. Harrison, L. R., East, A. E., Smith, D. P., Logan, J. B., Bond, R. M., Nicol, C. L., ... & Luna, L. (2018). River response to large-dam removal in a Mediterranean hydroclimatic setting: Carmel River, California, USA. *Earth Surface Processes and Landforms*, *43*(15), 3009-3021.
36. Haug, M. D., Sauer, E. K., & Fredlund, D. G. (1977). Retrogressive slope failures at Beaver Creek, south of Saskatoon, Saskatchewan, Canada. *Canadian Geotechnical Journal*, *14*(3), 288-301.
37. Holtz, R. D., & Kovacs, W. D. (1981). *An introduction to geotechnical engineering*. Englewood Cliffs, N.J: Prentice-Hall.
38. Huang, J., Greimann, B., & Kimbrel, S. (2019). Simulation of Sediment Flushing in Paonia Reservoir of Colorado. *Journal of Hydraulic Engineering*, *145(12)*, 06019015.
39. Ibrahim, H. A., & Brutsaert, W. (1965). Inflow hydrographs from large unconfined aquifers. *Journal of the Irrigation and Drainage Division*, *91*(2), 21-38.
40. Isaac, N., & Eldho, T. I. (2016). Sediment management studies of a run-of-the-river hydroelectric project using numerical and physical model simulations. *International journal of river basin management*, *14*(2), 165-175.
41. Kibler, K. M., Tullos, D. D., & Kondolf, G. M. (2011). Learning from dam removal monitoring: challenges to selecting experimental design and establishing significance of outcomes. *River Research and Applications*, *27*(8), 967-975.
42. Kondolf, G. M., Gao, Y., Annandale, G. W., Morris, G. L., Jiang, E., Zhang, J., ... & Hotchkiss, R. (2014). Sustainable sediment management in reservoirs and regulated rivers: Experiences from five continents. *Earth's Future*, *2*(5), 256-280.
43. Kosky, K. M., Straub, T. D., Roseboom, D. P., & Johnson, G. P. (2004). Preliminary results of a dam-removal analysis on brewster creek near st. Charles, Illinois, 2002-2004. In *Self-Sustaining Solutions for Streams, Wetlands, and Watersheds, 12-15, September 2004* (p. 48). American Society of Agricultural and Biological Engineers.
44. Krahn, J., Fredlund, D. G., & Klassen, M. J. (1989). Effect of soil suction on slope stability at Notch Hill. *Canadian Geotechnical Journal*, *26*(2), 269-278.
45. Lai, Y. G., & Wu, K. (2013). Modeling of vertical and lateral erosion on the Chosui River, Taiwan. In *World Environmental and Water Resources Congress 2013: Showcasing the Future* (pp. 1747-1756).
46. Lai, Y. (2014). Modeling of Delta Erosion during Elwha Dam Removal with SRH-2D. U.S. Bureau of Reclamation. Technical Report No. SRH-2014-31.
47. Langendoen, E. J., Simon, A., & Thomas, R. E. (2001). CONCEPTS-a process-based modeling tool to evaluate stream-corridor restoration designs. In Wetlands Engineering & River Restoration 2001 (pp. 1-11).

48. Lin, H., Zhong, W., Cao, P., & Liu, T. (2013). Variational safety factors and slip surfaces of slope using three-dimensional strength reduction analysis. *Journal of the Geological Society of India, 82*(5), 545-552.
49. Magilligan, F. J., Nislow, K. H., Kynard, B. E., & Hackman, A. M. (2016). Immediate changes in stream channel geomorphology, aquatic habitat, and fish assemblages following dam removal in a small upland catchment. *Geomorphology*, *252*, 158-170.
50. Magirl, C. S., Connolly, P. J., Coffin, B., Duda, J. J., & Draut, A. E. (2010). Sediment management strategies associated with dam removal in the State of Washington. In *2nd Joint Federal Interagency Conference*.
51. Maihemuti, B., Wang, E., Hudan, T., & Xu, Q. (2016). Numerical simulation analysis of reservoir bank fractured rock-slope deformation and failure processes. *International Journal of Geomechanics*, *16*(2), 04015058.
52. Major, JJ, O'Connor, JE, Podolak, CJ et al. (2012). Geomorphic response of the Sandy River, Oregon, to removal of Marmot Dam. US Geological Survey Professional Paper 1792, 64 pp.
53. Major, J. J., East, A. E., O'Connor, J. E., Grant, G. E., Wilcox, A. C., Magirl, C. S., ... & Tullos, D. D. (2017). Geomorphic responses to dam removal in the United States–a two-decade perspective. *Gravel-bed rivers*, *10*(9781118971437), 355-383.
54. Minear, J. T., & Kondolf, G. M. (2009). Estimating reservoir sedimentation rates at large spatial and temporal scales: A case study of California. *Water Resources Research, 45*(12).
55. Olsen, N. R. B., & Haun, S. (2018). Numerical modelling of bank failures during reservoir draw-down.
56. Pearson, A. J., Snyder, N. P., & Collins, M. J. (2011). Rates and processes of channel response to dam removal with a sand-filled impoundment. *Water Resources Research, 47*(8).
57. Pizzuto, J. (2002). Effects of Dam Removal on River Form and Process: Although many well-established concepts of fluvial geomorphology are relevant for evaluating the effects of dam removal, geomorphologists remain unable to forecast stream channel changes caused by the removal of specific dams. *BioScience*, *52*(8), 683-691.
58. Randle, Timothy J., et al. (2015) "Large-scale dam removal on the Elwha River, Washington, USA: Erosion of reservoir sediment." *Geomorphology,* 246, 709-728.
59. Randle, T. J., & Bountry, J. (2017). Dam Removal Analysis Guidelines for Sediment. *Washington, DC: US Department of the Interior, Bureau of Reclamation, Advisory Committee on Water Information, Subcommittee on Sedimentation.*
60. Randle, T., Kimbrel, S., Collins, K., Boyd, P., Jonas, M., Vermeeren, R., ... & Fripp, J. (2017). Frequently Asked Questions about Reservoir Sedimentation and Sustainability. Subcommittee on Sedimentation, National Reservoir Sedimentation and Sustainability.

61. Randle et al. (2019). Reservoir Sediment Management: Building a Legacy of Sustainable Water Storage Reservoirs. *National Reservoir Sedimentation and Sustainability Team White Paper*.
62. Reid, J. R. (1992, October). Mechanisms of shoreline erosion along lakes and reservoirs. In Proceedings, US Army Corps of Engineers Workshop on Reservoir Shoreline Erosion: A National Problem (pp. 18-32).
63. Rios, S., da Fonseca, A. V., Cristelo, N., & Pinheiro, C. (2017, July). Geotechnical Properties of Sediments by In Situ Tests. In *International Congress and Exhibition" Sustainable Civil Infrastructures: Innovative Infrastructure Geotechnology"* (pp. 59-68). Springer, Cham.
64. Ritchie, A. C., Warrick, J. A., East, A. E., Magirl, C. S., Stevens, A. W., Bountry, J. A., ... & Gelfenbaum, G. R. (2018). Morphodynamic evolution following sediment release from the world's largest dam removal. *Scientific reports*, *8*(1), 1-13.
65. Simon, A., Curini, A., Darby, S. E., & Langendoen, E. J. (2000). Bank and near-bank processes in an incised channel. *Geomorphology*, *35*(3-4), 193-217.
66. Singh, R. N., Ngah, S. A., & Atkins, A. S. (1985). Applicability of current groundwater theories for the prediction of water inflows to surface mining excavations. In *2nd International Mine Water Congress of IMWA, Mine Water, Granada Spain*(Vol. 1, pp. 553-569).
67. Stark, T. D., Choi, H., & McCone, S. (2005). Drained shear strength parameters for analysis of landslides. *Journal of Geotechnical and Geoenvironmental Engineering*, *131*(5), 575-588.
68. State Water Resources Control Board (2018). Environmental Impact Report for the Lower Klamath Project License Surrender Volume I. Available online at: https://www.waterboards.ca.gov/waterrights/water_issues/programs/water_quality_cert/docs/lower_klamath_ferc14803_deir/vol_1.pdf
69. Tullos, D. D., Finn, D. S., & Walter, C. (2014). Geomorphic and ecological disturbance and recovery from two small dams and their removal. *PLoS One*, *9*(9).
70. Tullos, D. D., Collins, M. J., Bellmore, J. R., Bountry, J. A., Connolly, P. J., Shafroth, P. B., & Wilcox, A. C. (2016). Synthesis of common management concerns associated with dam removal. JAWRA Journal of the American Water Resources Association, 52(5), 1179-1206.
71. Wilcox, A. C., O'Connor, J. E., & Major, J. J. (2014). Rapid reservoir erosion, hyperconcentrated flow, and downstream deposition triggered by breaching of 38 m tall Condit Dam, White Salmon River, Washington. *Journal of Geophysical Research: Earth Surface*, *119*(6), 1376-139
72. Yu, H. S., Salgado, R., Sloan, S. W., & Kim, J. M. (1998). Limit analysis versus limit equilibrium for slope stability. *Journal of Geotechnical and Geoenvironmental Engineering*, *124*(1), 1-11.
73. Zhan, T. L., Zhang, W. J., & Chen, Y. M. (2006). Influence of reservoir level change on slope stability of a silty soil bank. In Unsaturated Soils 2006 (pp. 463-472).

APPENDICES

# A. Geotechnical Failure Verification

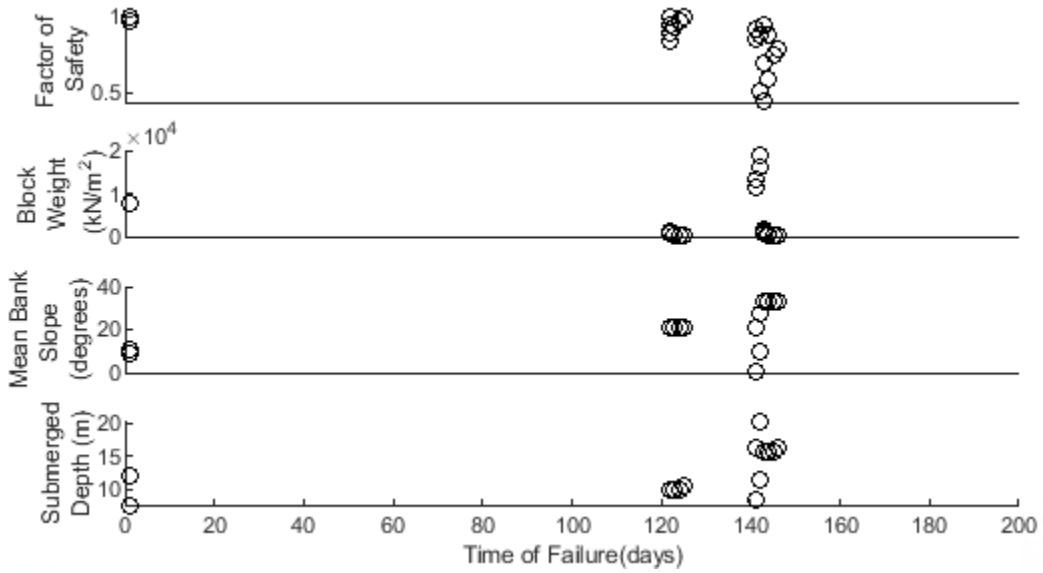


**Figure 1.** Comparison of parameters used to calculate geotechnical failure for the Lake Aldwell reservoir cross section during Staged-Short drawdown.

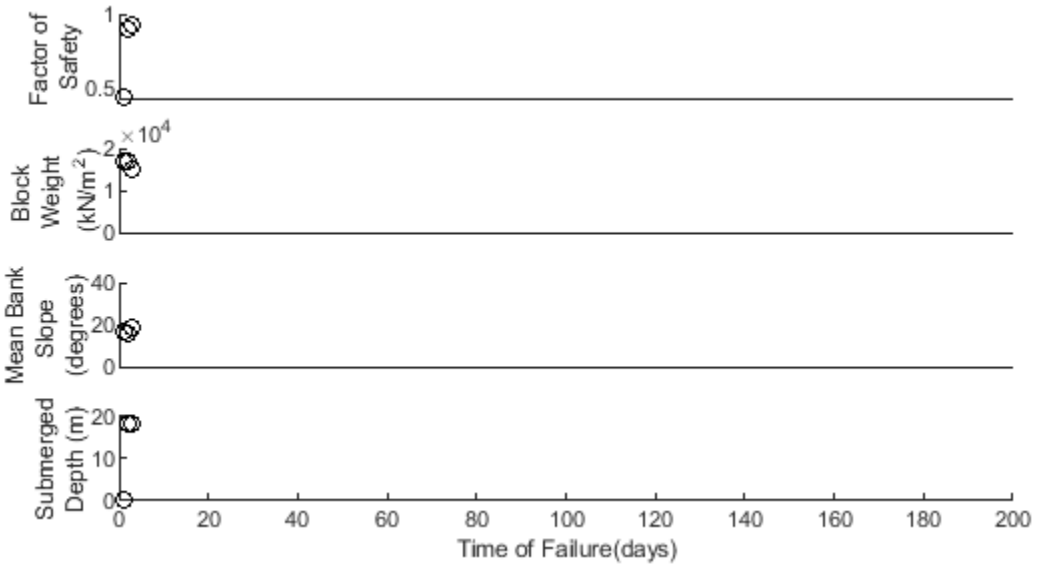


**Figure 2.** Comparison of parameters used to calculate geotechnical failure for the Lake Aldwell reservoir cross section during Rapid drawdown.